Preprints of the 23rd IFAC World Congress
Busan, Republic of Korea, August 23-28, 2026

Interval Estimation for Bounded Jacobian Nonlinear Systems by Zonotope Analysis ⋆

Chi Xu * **Zhenhua Wang** * **Nacim Meslem** ** **Tarek Raïssi** *** **Yacine Chitour** ****

* *Department of Control Science and Engineering, Harbin Institute of Technology, Harbin, 150001 P. R. China, (e-mail: chi.xu@stu.hit.edu.cn, zhenhua.wang@hit.edu.cn).*
** *University Grenoble Alpes, CNRS, Grenoble INP, GIPSA-lab, F-38000 Grenoble, France , (e-mail: nacim.meslem@grenoble-inp.fr)*
*** *Conservatoire National des Arts et Métiers (CNAM), 292 Rue Saint-Martin, 75141 Paris, France,(e-mail: tarek.raissi@cnam.fr)*
**** *Université Paris-Saclay, CNRS, CentraleSupélec, Laboratoire des Signaux et Systèmes, 91190 Gif sur-Yvette, France, and also with Fédération de Mathématiques de CentraleSupélec, 91190 Gif-sur-Yvette, France (e-mail: yacine.chitour@centralesupelec.fr)*

Abstract: This paper introduces an interval state estimation method for discrete-time bounded Jacobian nonlinear systems allying Luenberger-like observer with zonotope set computation. First, a robust observer is designed to obtain bounded-error and point-estimation with a peak-to-peak performance. This allows one to cope with the unknown but bounded process disturbance and measurement noise. Then, based on the stable dynamics of the observation error, tight interval estimation is obtained by applying zonotope set computation and analysis. To sum up, a comprehensive interval estimation algorithm is proposed by integrating the robust (in the sense of peak-to-peak performance index) point-valued estimate with the feasible zonotope set of the estimation error. Numerical simulation tests are conducted to assess the effectiveness of the proposed approach.

Keywords: Interval estimation, nonlinear system, zonotope, observer design.

1. INTRODUCTION

The knowledge of the internal state of dynamics systems is essential in many engineering applications, including systems monitoring, fault detection, and state feedback control Wang and Shen (2023). Due to uncertainties such as process disturbances and measurement noise, the estimated state of a system may not align perfectly with its actual one. A solution to solve this problem (to get a reliable estimation) can be obtained by assuming that the uncertain parts of the system are unknown but bounded and then using interval computation techniques to design set-valued state estimators. It is worth pointing out that compared to the stochastic assumption, that is the existence of probability distribution functions describing the system uncertainties, the unknown but bounded assumption is more natural and easier to meet in real world systems.

In the literature, interval estimation techniques can be divided into two main categories, interval observer-based methods Li et al. (2019); Tahir and Açıkmeşe (2021); Khajenejad and Yong (2022) and set-based methods Wang et al. (2018); Zhang et al. (2021); Wang et al. (2024). Using the monotone systems theory, the interval observer-based methods aim to design two sub-observers to ensure the stability and positivity of the estimation error, and provide two bounds framing the system state Raïssi et al. (2011). However, sometimes the design condition of interval observers is too restrictive to find suitable gain matrices in the sense of estimation performance, which limits their application. Although using coordinate transformation can relax the design condition, the transformation introduces additional conservatism and reduces the estimation accuracy.

Unlike interval observers, the main idea of set-based methods is to construct, step-by-step, geometrical sets that contain the reachable state of the system Althoff and Rath (2021). Ellipsoids, polytopes and zonotopes are commonly used as geometrical sets. Owing of their geometrical and computational properties, zonotope-based methods provide a favorable balance between estimation accuracy and computational efficiency Tang et al. (2019). For nonlinear discrete-time systems, the authors of Alamo et al. (2005) have proposed a zonotope-based interval state estimator based on an adaptation of the prediction/correction principle to the set-membership paradigm. Unluckily, the convergence rate of the estimation error of this approach is not tunable and there is no proof of its stability Efimov et al. (2013). For the case of linear time-invariant systems (LTI), the authors of Tang et al. (2019) have developed an effi-

⋆ This work was supported by the National Natural Science Foundation of China under Grant No. 62373125.

©2026 the authors. Accepted by IFAC for publication under a Creative Commons Licence CC-BY-NC-ND

cient two-step set-valued estimation method by coupling a point-wise observer scheme with zonotope analysis of the estimation error. Unfortunately, the application scope of this method is limited to the case of linear systems and cannot be directly extended to the case of nonlinear systems.

To overcome the limitations of the aforementioned works, we propose an interval estimation method that combines a point estimation observer with zonotope analysis of the estimation error for bounded Jacobian nonlinear systems. The key contributions of this work are as follows:

(1) A bounded-error observer is constructed to obtain point estimates with guaranteed peak-to-peak performance. In fact, the proposed design method for the observer gain allows one attenuating the negative effects of the unknown but bounded state disturbance and measurement noise on the estimation error.
(2) By using the available bounds on the state disturbances and measurement noise, online zonotope computations are applied to design a comprehensive set-valued state estimator. Compared with the existing methods [3], the proposed state estimator provides results that are more accurate.

The remainder of this paper is organized as follows. Section 2 introduces some preliminaries and problem formulation. In Section 3, a comprehensive interval estimation method is introduced based on a bounded-error observer design and a zonotope analysis. To illustrate the effectiveness of the proposed method, numerical simulation results are given and commented in Section 4. A conclusion and some perspectives of this work are presented in Section 5.

2. PRELIMINARIES AND PROBLEM FORMULATION

2.1 Preliminaries

Notation: $\mathbb{R}^n$ denotes the n-dimensional Euclidean space. $\mathbb{R}^{m\times n}$ is the set of matrices of size m by n. $\oplus$ stands for the Minkowski sum. $(\cdot)^{\mathrm{T}}$ represents the transpose of a matrix/vector. In a symmetric matrix, asterisk $*$ stands for the symmetric term. $\min(\cdot)$, $\max(\cdot)$, $\leq, <, \geq, >$ and $|\cdot|$ should be understood elementwise. For a vector $\boldsymbol{z} \in \mathbb{R}^n$, $\boldsymbol{z}(i)$ is its i-th element, $\|\boldsymbol{z}\|_1 = \sum_i^n |\boldsymbol{z}(i)|$, $\|\boldsymbol{z}\|_2 = \sqrt{\boldsymbol{z}^{\mathrm{T}}\boldsymbol{z}}$, $\mathrm{diag}(\boldsymbol{z})$ represents a diagonal matrix with the entries of $\boldsymbol{z}$ as its diagonal elements. $\downarrow_q(\cdot)$, introduced in the Appendix, denotes a zonotope reduction operator. An interval $[\boldsymbol{z}] \triangleq [\underline{\boldsymbol{z}}, \overline{\boldsymbol{z}}]$ is a set of vectors $\boldsymbol{z}$ satisfying $\underline{\boldsymbol{z}} \leq \boldsymbol{z} \leq \overline{\boldsymbol{z}}$. For a matrix $\boldsymbol{G} \in \mathbb{R}^{n\times m}$, $\boldsymbol{G}(i,j)$ is its (i,j)-th element, $\boldsymbol{G} \succ \boldsymbol{0} (\prec \boldsymbol{0})$ means that $\boldsymbol{G}$ is a positive (negative) definite matrix and an interval matrix $[\boldsymbol{G}] \triangleq [\underline{\boldsymbol{G}}, \overline{\boldsymbol{G}}]$ is a set of matrices $\boldsymbol{G}$ which satisfy $\underline{\boldsymbol{G}}(i,j) \leq \boldsymbol{G}(i,j) \leq \overline{\boldsymbol{G}}(i,j), i = 1,\ldots,n, j = 1,\ldots,m$. $\boldsymbol{I}_n$ represents the $n \times n$ identity matrix, while $\boldsymbol{0}$ denotes a zero matrix or vector of appropriate dimensions.

Definition 1. An m-order zonotope $\mathcal{Z} \subseteq \mathbb{R}^n$ is defined as:

$$\mathcal{Z} = \boldsymbol{p} \oplus \boldsymbol{G}\mathcal{B}^m = \{\boldsymbol{p} + \boldsymbol{G}\xi, \xi \in \mathcal{B}^m, \mathcal{B}^m = [-1,1]^m\} \quad (1)$$

with $\boldsymbol{p} \in \mathbb{R}^n$ and $\boldsymbol{G}$. For notational simplicity, a zonotope will be denoted by $\mathcal{Z} = \langle \boldsymbol{p}, \boldsymbol{G}\rangle$ in the sequel.

Property 1. Tang et al. (2020) Given zonotopes $\langle \boldsymbol{p}, \boldsymbol{G}\rangle$, $\langle \boldsymbol{p}_1, \boldsymbol{G}_1\rangle$, $\langle \boldsymbol{p}_2, \boldsymbol{G}_2\rangle \subseteq \mathbb{R}^n$, $\boldsymbol{A} \in \mathbb{R}^{l\times n}$ and $\boldsymbol{z} \in \mathbb{R}^n$ one has:

$$\boldsymbol{A}\langle \boldsymbol{p}, \boldsymbol{G}\rangle \oplus \boldsymbol{z} = \langle \boldsymbol{A}\boldsymbol{p} + \boldsymbol{z}, \boldsymbol{A}\boldsymbol{M}\rangle \quad (2)$$

$$\boldsymbol{x} \in \langle \boldsymbol{p}, \boldsymbol{G}\rangle \subseteq [\underline{\boldsymbol{x}}, \overline{\boldsymbol{x}}] \quad (3)$$

$$\langle \boldsymbol{p}, \boldsymbol{G}\rangle \subseteq \langle \boldsymbol{p}, \downarrow_q (\boldsymbol{G})\rangle \quad (4)$$

$$\langle \boldsymbol{p}_1, \boldsymbol{G}_1\rangle \oplus \langle \boldsymbol{p}_2, \boldsymbol{G}_2\rangle = \langle \boldsymbol{p}_1 + \boldsymbol{p}_2, [\boldsymbol{G}_1 \ \ \boldsymbol{G}_2]\rangle \quad (5)$$

where $\boldsymbol{p}, \boldsymbol{p}_1, \boldsymbol{p}_2 \in \mathbb{R}^n$, $\boldsymbol{G} \in \mathbb{R}^{n\times m}, \boldsymbol{G}_1 \in \mathbb{R}^{n\times m_1}, \boldsymbol{G}_2 \in \mathbb{R}^{n\times m_2}$. $\downarrow_q(\cdot)$ is a zonotope reduction operator and q is a integer satisfying $n < q < m$. In addition, the bounds of $\boldsymbol{x}$ are obtained by

$$i = 1,\ldots,n, \begin{cases} \underline{\boldsymbol{x}}(i) = \boldsymbol{p}(i) - \|\boldsymbol{G}(i,:)\|_1 \\ \overline{\boldsymbol{x}}(i) = \boldsymbol{p}(i) + \|\boldsymbol{G}(i,:)\|_1 \end{cases}, \quad (6)$$

Lemma 1. De Oliveira et al. (1999) Given a matrix $\boldsymbol{G} \succ \boldsymbol{0}$ and matrices $\boldsymbol{N}, \boldsymbol{Q}, \boldsymbol{O}$, the following statements are equivalent:

$$\boldsymbol{Q}^{\mathrm{T}}\boldsymbol{G}\boldsymbol{Q} - \boldsymbol{N} \prec \boldsymbol{0} \Leftrightarrow \begin{bmatrix} -\boldsymbol{N} & * \\ \boldsymbol{U}\boldsymbol{Q} & \boldsymbol{G} - \boldsymbol{O} - \boldsymbol{O}^{\mathrm{T}} \end{bmatrix} \prec \boldsymbol{0} \quad (7)$$

Lemma 2. Alamo et al. (2005) Given a vector $\boldsymbol{p} \in \mathbb{R}^n$ and an interval matrix $[\boldsymbol{G}] = [\underline{\boldsymbol{G}}, \overline{\boldsymbol{G}}] \subseteq \mathbb{R}^{n\times m}$, a family of zonotopes is represented by $\mathcal{Z} = \boldsymbol{p} \oplus [\boldsymbol{G}]\mathcal{B}^m$. A zonotope inclusion, denoted by $\Diamond\mathcal{Z}$, is a zonotope enclosing $\mathcal{Z}$ and can be computed as follows:

$$\mathcal{Z} \subset \Diamond\mathcal{Z} = \boldsymbol{p} \oplus \left[\boldsymbol{D}^{\boldsymbol{c}}_{[\boldsymbol{G}]}, \boldsymbol{D}^{\boldsymbol{s}}_{[\boldsymbol{G}]}\right]\mathcal{B}^{m+n} = \langle \boldsymbol{p}, \left[\boldsymbol{D}^{\boldsymbol{c}}_{[\boldsymbol{G}]}, \boldsymbol{D}^{\boldsymbol{s}}_{[\boldsymbol{G}]}\right]\rangle \quad (8)$$

where $\boldsymbol{D}^{c}_{[\boldsymbol{G}]} \in \mathbb{R}^{n\times m}$, $\boldsymbol{D}^{s}_{[\boldsymbol{G}]} \in \mathbb{R}^{n\times n}$ are matrices related to $[\boldsymbol{G}]$ which are defined by:

$$\begin{aligned} \boldsymbol{D}^{c}_{[\boldsymbol{G}]} &= \frac{\underline{\boldsymbol{G}} + \overline{\boldsymbol{G}}}{2}, \ \boldsymbol{R}^{c}_{[\boldsymbol{G}]} = \frac{\overline{\boldsymbol{G}} - \underline{\boldsymbol{G}}}{2}, \\ \boldsymbol{s}_{[\boldsymbol{G}]}(i) &= \|\boldsymbol{R}^{c}_{[\boldsymbol{G}]}(i,:)\|_1, \ i,\ldots,n, \\ \boldsymbol{D}^{s}_{[\boldsymbol{G}]} &= \mathrm{diag}(\boldsymbol{s}_{[\boldsymbol{G}]}). \end{aligned} \quad (9)$$

2.2 Problem statement

Consider a discrete-time nonlinear system described by

$$\begin{cases} \boldsymbol{x}_{k+1} = \boldsymbol{A}\boldsymbol{x}_k + \boldsymbol{B}\boldsymbol{u}_k + \boldsymbol{f}(\boldsymbol{x}_k) + \boldsymbol{D}_1\boldsymbol{w}_k \\ \boldsymbol{y}_k = \boldsymbol{C}\boldsymbol{x}_k + \boldsymbol{D}_2\boldsymbol{v}_k \end{cases} \quad (10)$$

where $\boldsymbol{x}_k \in \mathbb{R}^{n_x}$, $\boldsymbol{y}_k \in \mathbb{R}^{n_y}$, $\boldsymbol{u}_k \in \mathbb{R}^{n_u}$, $\boldsymbol{w}_k \in \mathbb{R}^{n_w}$ and $\boldsymbol{v}_k \in \mathbb{R}^{n_v}$ are the system state, the measurement output, the control input, the process disturbance, and the measurement noise, respectively. $\boldsymbol{A}, \boldsymbol{B}, \boldsymbol{C}, \boldsymbol{D}_1, \boldsymbol{D}_2$ are known matrices with suitable dimensions. $\boldsymbol{f}(\cdot) : \mathbb{R}^{n_x} \to \mathbb{R}^{n_x}$ is a nonlinear function that is first-order differentiable with respect to $\boldsymbol{x}$.

Assumption 1. Let $\mathcal{Z} \subseteq \mathbb{R}^{n_x}$ be the admissible domain of $\boldsymbol{x}$. It is assumed that known matrices $\underline{\boldsymbol{M}}, \overline{\boldsymbol{M}} \in \mathbb{R}^{n_x\times n_x}$ exist such that, for all $\boldsymbol{x} \in \mathcal{Z}$, the Jacobian of $\boldsymbol{f}(\cdot)$ satisfies

$$\underline{\boldsymbol{M}} \leq \frac{\partial \boldsymbol{f}}{\partial \boldsymbol{x}}(\boldsymbol{x}) \leq \overline{\boldsymbol{M}}. \quad (11)$$

Under Assumption 1, for any $\boldsymbol{z}_1, \boldsymbol{z}_2 \in \mathcal{Z}$, there exists a matrix $\boldsymbol{M} \in [\underline{\boldsymbol{M}}, \overline{\boldsymbol{M}}]$ such that

$$\Delta\boldsymbol{f}^{\mathrm{T}}(\boldsymbol{z}_1 - \boldsymbol{z}_2) \leq (\boldsymbol{z}_1 - \boldsymbol{z}_2)^{\mathrm{T}}\boldsymbol{M}(\boldsymbol{z}_1 - \boldsymbol{z}_2), \quad (12)$$

$$\Delta\boldsymbol{f}^{\mathrm{T}}\Delta\boldsymbol{f} \leq (\boldsymbol{z}_1 - \boldsymbol{z}_2)^{\mathrm{T}}\boldsymbol{M}^{\mathrm{T}}\boldsymbol{M}(\boldsymbol{z}_1 - \boldsymbol{z}_2), \quad (13)$$

where $\Delta\boldsymbol{f} = \boldsymbol{f}(\boldsymbol{z}_1) - \boldsymbol{f}(\boldsymbol{z}_2)$.

Assumption 2. It is assumed that the process disturbance $\boldsymbol{w}_k$, measurement noise $\boldsymbol{v}_k$, and initial state $\boldsymbol{x}_0$ are unknown but bounded as follows:

$$\forall\ k \geq 0, \ |\boldsymbol{w}_k| \leq \overline{\boldsymbol{w}}, \ |\boldsymbol{v}_k| \leq \overline{\boldsymbol{v}}, \ |\boldsymbol{x}_0 - \boldsymbol{p}_0| \leq \overline{\boldsymbol{x}}_0, \quad (14)$$

where $\overline{\boldsymbol{w}} \in \mathbb{R}^{n_w}, \overline{\boldsymbol{v}} \in \mathbb{R}^{n_v}$, $\overline{\boldsymbol{x}}_0 \in \mathbb{R}^{n_x}$ and $\boldsymbol{p}_0 \in \mathbb{R}^{n_x}$ are known. Using (1), (14) can be rewritten as

$$\begin{aligned} \boldsymbol{w}_k &\in \mathcal{W} = \langle \boldsymbol{0}, \boldsymbol{G}_w \rangle, \boldsymbol{v}_k \in \mathcal{V} = \langle \boldsymbol{0}, \boldsymbol{G}_v \rangle, \\ \boldsymbol{x}_0 &\in \mathcal{Z}_0 = \langle \boldsymbol{p}_0, \boldsymbol{G}_{\boldsymbol{x},0} \rangle, \end{aligned} \tag{15}$$

where $\boldsymbol{G}_w = \mathrm{diag}(\overline{\boldsymbol{w}})$, $\boldsymbol{G}_v = \mathrm{diag}(\overline{\boldsymbol{v}})$, $\boldsymbol{G}_{\boldsymbol{x},0} = \mathrm{diag}(\overline{\boldsymbol{x}}_0)$.

This paper aims at designing a set-valued state estimator for system (11) that computes, in real-time, a tight interval $[\underline{\boldsymbol{x}}, \overline{\boldsymbol{x}}]$ that contains the actual state vector of the system.

3. MAIN RESULT

In this section, a robust observer is designed to provide point-estimation in the bounded-error context with peak-to-peak performance index. Then, a comprehensive interval estimation method is proposed by combining the point-estimate and zonotope analysis of the reachable set of the estimation error.

3.1 An offline Bounded-error Observer Design

Consider the following observer

$$\hat{\boldsymbol{x}}_{k+1} = \boldsymbol{A}\hat{\boldsymbol{x}}_k + \boldsymbol{B}\boldsymbol{u}_k + \boldsymbol{f}(\hat{\boldsymbol{x}}_k) + \boldsymbol{L}(\boldsymbol{y}_k - \boldsymbol{C}\hat{\boldsymbol{x}}_k) \tag{16}$$

where $\hat{\boldsymbol{x}} \in \mathbb{R}^{n_x}$ and $\boldsymbol{L} \in \mathbb{R}^{n_x \times n_y}$ are the estimated state and observer gain.

The estimation error is defined as:

$$\boldsymbol{e}_k = \boldsymbol{x}_k - \hat{\boldsymbol{x}}_k. \tag{17}$$

By substituting (10) and (16) into (17), we have

$$\boldsymbol{e}_{k+1} = \tilde{\boldsymbol{A}}\boldsymbol{e}_k + \Delta\boldsymbol{f}_k + \boldsymbol{D}_1\boldsymbol{w}_k - \boldsymbol{L}\boldsymbol{D}_2\boldsymbol{v}_k \tag{18}$$

with $\tilde{\boldsymbol{A}} = \boldsymbol{A} - \boldsymbol{L}\boldsymbol{C}$, $\Delta\boldsymbol{f}_k = \boldsymbol{f}(\boldsymbol{x}_k) - \boldsymbol{f}(\hat{\boldsymbol{x}}_k)$.

Theorem 1. For a given constant $0 < \lambda < 1$, suppose there exist constants $a > 0$, $b > 0$, $\gamma > 0$, $\mu_w > 0$, $\mu_v > 0$, a positive definite matrix $\boldsymbol{P} \succ \boldsymbol{0} \in \mathbb{R}^{n_x \times n_x}$, matrices $\boldsymbol{W} \in \mathbb{R}^{n_x \times n_y}$, $\boldsymbol{U} \in \mathbb{R}^{n_x \times n_y}$, such that for all $\boldsymbol{M} \in [\underline{\boldsymbol{M}}, \overline{\boldsymbol{M}}]$, the following inequalities hold:

$$\begin{bmatrix} \boldsymbol{\Phi}_{11} & * & * & * & * & * \\ -a\boldsymbol{I} & -b\boldsymbol{I}_{n_x} & * & * & * & * \\ \boldsymbol{0} & \boldsymbol{0} & -\gamma\boldsymbol{I}_{n_w} & * & * & * \\ \boldsymbol{0} & \boldsymbol{0} & \boldsymbol{0} & -\gamma\boldsymbol{I}_{n_v} & * & * \\ \boldsymbol{\Phi}_{51} & \boldsymbol{P} & \boldsymbol{P}\boldsymbol{D}_1 & -\boldsymbol{W}\boldsymbol{D}_2 & -\boldsymbol{P} & * \\ \boldsymbol{U}\boldsymbol{J} & \boldsymbol{0} & \boldsymbol{0} & \boldsymbol{0} & \boldsymbol{0} & \boldsymbol{\Phi}_{66} \end{bmatrix} \prec \boldsymbol{0}, \tag{19}$$

$$\begin{bmatrix} \lambda\boldsymbol{P} & * & * & * \\ \boldsymbol{0} & (\mu_w - \gamma)\boldsymbol{I}_{n_w} & * & * \\ \boldsymbol{0} & \boldsymbol{0} & (\mu_v - \gamma)\boldsymbol{I}_{n_v} & * \\ \boldsymbol{I}_{n_x} & \boldsymbol{0} & \boldsymbol{0} & \mu\boldsymbol{I}_{n_x} \end{bmatrix} \succ \boldsymbol{0}, \tag{20}$$

where

$$\boldsymbol{\Phi}_{11} = \lambda\boldsymbol{P} - \boldsymbol{P} + a(\boldsymbol{M} + \boldsymbol{M}^{\mathrm{T}}),\ \boldsymbol{\Phi}_{51} = \boldsymbol{P}\boldsymbol{A} - \boldsymbol{W}\boldsymbol{C},$$

$$\boldsymbol{\Phi}_{66} = b\boldsymbol{I} - \boldsymbol{U} - \boldsymbol{U}^{\mathrm{T}},\ \mu = \mu_w + \mu_v.$$

Then, the estimation error dynamics (18) is input-to-state stable and its solution satisfies the peak-to-peak performance bound:

$$\|\boldsymbol{e}_k\|_2 \leq \sqrt{\mu\left(\lambda(1-\lambda)^k V_0 + \mu_w \overline{\boldsymbol{w}}^2 + \mu_v \overline{\boldsymbol{v}}^2\right)}, \tag{21}$$

where $V_0 = \boldsymbol{e}_0^{\mathrm{T}}\boldsymbol{P}\boldsymbol{e}_0$ and μ quantifies the attenuation level.

Thus, optimal estimation performance can be obtained by solving the following minimization problem:

$$\min_{a,b,\gamma,\mu_w,\mu_v,\boldsymbol{P},\boldsymbol{W},\boldsymbol{U}} \mu \quad \text{s. t.} \quad (19), (20). \tag{22}$$

If problem (22) is feasible, the observer gain matrix $\boldsymbol{L}$ is given by $\boldsymbol{L} = \boldsymbol{P}^{-1}\boldsymbol{W}$.

Proof: Firstly, using the positive definite matrix $\boldsymbol{P} \succ \boldsymbol{0}$, we define the following Lyapunov function $V_k = \boldsymbol{e}_k^{\mathrm{T}}\boldsymbol{P}\boldsymbol{e}_k$ and its time variation is described by

$$\Delta V_k = V_{k+1} - V_k = \boldsymbol{\zeta}_k^{\mathrm{T}}\boldsymbol{\Psi}\boldsymbol{\zeta}_k \tag{23}$$

where

$$\boldsymbol{\zeta}_k = \begin{bmatrix} \boldsymbol{e}_k \\ \Delta\boldsymbol{f}_k \\ \boldsymbol{w}_k \\ \boldsymbol{v}_k \end{bmatrix},\ \boldsymbol{\Psi} = \begin{bmatrix} \Psi_{11} & * & * & * \\ \Psi_{21} & \Psi_{22} & * & * \\ \Psi_{31} & \Psi_{32} & \Psi_{33} & * \\ \Psi_{41} & \Psi_{42} & \Psi_{43} & \Psi_{44} \end{bmatrix},$$

$$\Psi_{11} = \tilde{\boldsymbol{A}}^{\mathrm{T}}\boldsymbol{P}\tilde{\boldsymbol{A}} - \boldsymbol{P},\ \Psi_{21} = \boldsymbol{P}\tilde{\boldsymbol{A}},\ \Psi_{22} = \boldsymbol{P},$$

$$\Psi_{31} = \boldsymbol{D}_1^{\mathrm{T}}\boldsymbol{P}\tilde{\boldsymbol{A}},\ \Psi_{32} = \boldsymbol{D}_1^{\mathrm{T}}\boldsymbol{P},\ \Psi_{33} = \boldsymbol{D}_1^{\mathrm{T}}\boldsymbol{P}\boldsymbol{D}_1,$$

$$\Psi_{41} = (-\boldsymbol{L}\boldsymbol{D}_2)^{\mathrm{T}}\boldsymbol{P}\tilde{\boldsymbol{A}},\ \Psi_{42} = (-\boldsymbol{L}\boldsymbol{D}_2)^{\mathrm{T}}\boldsymbol{P},$$

$$\Psi_{43} = (-\boldsymbol{L}\boldsymbol{D}_2)^{\mathrm{T}}\boldsymbol{P}\boldsymbol{D}_1,\ \Psi_{44} = (-\boldsymbol{L}\boldsymbol{D}_2)^{\mathrm{T}}\boldsymbol{P}(-\boldsymbol{L}\boldsymbol{D}_2).$$

Then, using Lemma 1 and substituting $\boldsymbol{W} = \boldsymbol{P}\boldsymbol{L}$ into (19), it yields

$$\begin{bmatrix} \boldsymbol{\Gamma}_{11} & * & * & * & * \\ -a\boldsymbol{I} & -b\boldsymbol{I}_{n_x} & * & * & * \\ \boldsymbol{0} & \boldsymbol{0} & -\gamma_l\boldsymbol{I}_{n_w} & * & * \\ \boldsymbol{0} & \boldsymbol{0} & \boldsymbol{0} & -\gamma_l\boldsymbol{I}_{n_v} & * \\ \boldsymbol{\Gamma}_{51} & \boldsymbol{P} & \boldsymbol{P}\boldsymbol{D}_1 & -\boldsymbol{W}\boldsymbol{D}_2 & -\boldsymbol{P} \end{bmatrix} \prec \boldsymbol{0} \tag{24}$$

where

$$\boldsymbol{\Gamma}_{11} = \lambda_l\boldsymbol{P} - \boldsymbol{P} + a(\boldsymbol{M} + \boldsymbol{M}^{\mathrm{T}}) + b\boldsymbol{M}^{\mathrm{T}}\boldsymbol{M},$$
$$\boldsymbol{\Gamma}_{51} = \boldsymbol{P}(\boldsymbol{A} - \boldsymbol{L}\boldsymbol{C}).$$

Using the Schur complement lemma Boyd and Vandenberghe (2004), (24) can be rewritten as

$$\boldsymbol{\Psi} + \begin{bmatrix} \Xi_{11} & * & * & * \\ -a\boldsymbol{I} & -b\boldsymbol{I}_{n_x} & * & * \\ \boldsymbol{0} & \boldsymbol{0} & -\gamma_l\boldsymbol{I}_{nw} & * \\ \boldsymbol{0} & \boldsymbol{0} & \boldsymbol{0} & -\gamma_l\boldsymbol{I}_{nv} \end{bmatrix} \prec \boldsymbol{0} \tag{25}$$

where $\Xi_{11} = \lambda_l\boldsymbol{P} + a(\boldsymbol{M} + \boldsymbol{M}^{\mathrm{T}}) + b\boldsymbol{M}^{\mathrm{T}}\boldsymbol{M}$

Pre- and post-multiplying (25) with $\boldsymbol{\zeta}_k^{\mathrm{T}}$ and its transpose yields

$$\Delta V_k + \lambda_l V_k - \gamma_l\boldsymbol{w}_k^{\mathrm{T}}\boldsymbol{w}_k - \gamma_l\boldsymbol{v}_k^{\mathrm{T}}\boldsymbol{v}_k + \alpha + \beta \leq 0 \tag{26}$$

where $\alpha = a\boldsymbol{e}_k^{\mathrm{T}}(\boldsymbol{M} + \boldsymbol{M}^{\mathrm{T}})\boldsymbol{e}_k - a\Delta\boldsymbol{f}_k^{\mathrm{T}}\boldsymbol{e}_k - a\boldsymbol{e}_k^{\mathrm{T}}\Delta\boldsymbol{f}_k$, $\beta = b\boldsymbol{e}_k^{\mathrm{T}}\boldsymbol{M}^{\mathrm{T}}\boldsymbol{M}\boldsymbol{e}_k - b\Delta\boldsymbol{f}_k^{\mathrm{T}}\Delta\boldsymbol{f}_k$. Therefore, the satisfaction of (19) implies that (26) holds.

Subsequently, based on (12) and $a > 0$, it follows that

$$\begin{aligned} \Delta\boldsymbol{f}_k^{\mathrm{T}}(\boldsymbol{x}_k - \hat{\boldsymbol{x}}_k) &\leq (\boldsymbol{x}_k - \hat{\boldsymbol{x}}_k)^{\mathrm{T}}\boldsymbol{M}(\boldsymbol{x}_k - \hat{\boldsymbol{x}}_k) \\ \Delta\boldsymbol{f}_k^{\mathrm{T}}\boldsymbol{e}_k + \boldsymbol{e}_k^{\mathrm{T}}\Delta\boldsymbol{f}_k &\leq \boldsymbol{e}_k^{\mathrm{T}}(\boldsymbol{M} + \boldsymbol{M}^{\mathrm{T}})\boldsymbol{e}_k \\ \alpha &\geq 0 \end{aligned} \tag{27}$$

Similarly, based on (13) and $b > 0$, we have

$$\begin{aligned} \Delta\boldsymbol{f}_k^{\mathrm{T}}\Delta\boldsymbol{f}_k &\leq (\boldsymbol{x}_k - \hat{\boldsymbol{x}}_k)^{\mathrm{T}}\boldsymbol{M}^{\mathrm{T}}\boldsymbol{M}(\boldsymbol{x}_k - \hat{\boldsymbol{x}}_k) \\ \Delta\boldsymbol{f}_k^{\mathrm{T}}\Delta\boldsymbol{f}_k &\leq \boldsymbol{e}_k^{\mathrm{T}}\boldsymbol{M}^{\mathrm{T}}\boldsymbol{M}\boldsymbol{e}_k \\ \beta &\geq 0 \end{aligned} \tag{28}$$

According to (27) and (28), (26) becomes

$$\Delta V_k + \lambda_l V_k - \gamma_l\boldsymbol{w}_k^{\mathrm{T}}\boldsymbol{w}_k - \gamma_l\boldsymbol{v}_k^{\mathrm{T}}\boldsymbol{v}_k \leq 0 \tag{29}$$

When $\boldsymbol{w}_k = 0$ and $\boldsymbol{v}_k = 0$, we obtain $\Delta V_k \leq -\lambda_l V_k < 0$, which proves the global asymptotic stability of the

dynamics of the estimation error (18). Moreover, (29) can be reformulated as:

$$\begin{aligned} V_{k+1} &\leq (1-\lambda_l)V_k + \gamma_l \boldsymbol{w}_k^{\mathrm{T}}\boldsymbol{w}_k + \gamma_l \boldsymbol{v}_k^{\mathrm{T}}\boldsymbol{v}_k \\ &\leq (1-\lambda_l)V_k + \gamma_l \overline{\boldsymbol{w}}^{\mathrm{T}}\overline{\boldsymbol{w}} + \gamma_l \overline{\boldsymbol{v}}^{\mathrm{T}}\overline{\boldsymbol{v}} \end{aligned} \tag{30}$$

which leads to

$$\begin{aligned} V_k &\leq (1-\lambda_l)^k V_0 + \gamma_l \sum_{i=0}^{k-1}(1-\lambda_l)^i(\overline{\boldsymbol{w}}^{\mathrm{T}}\overline{\boldsymbol{w}} + \overline{\boldsymbol{v}}^{\mathrm{T}}\overline{\boldsymbol{v}}) \\ &< (1-\lambda_l)^k V_0 + \frac{\gamma_l}{\lambda_l}(\overline{\boldsymbol{w}}^{\mathrm{T}}\overline{\boldsymbol{w}} + \overline{\boldsymbol{v}}^{\mathrm{T}}\overline{\boldsymbol{v}}) \end{aligned} \tag{31}$$

Next, we apply Schur complement lemma to (20), which can be rewritten as

$$\boldsymbol{\Upsilon} - \mu^{-1}\boldsymbol{Y}^{\top}\boldsymbol{Y} \succ \boldsymbol{0} \tag{32}$$

where $\boldsymbol{\Upsilon} = \mathrm{diag}([\lambda_l \boldsymbol{P}, (\mu_w - \gamma_l)\boldsymbol{I}_{nw}, (\mu_v - \gamma_l)\boldsymbol{I}_{nv}])$, $\boldsymbol{Y} = [\boldsymbol{I}_{n_x}\ \boldsymbol{0}\ \boldsymbol{0}]$. Pre- and post-multiplying (32) by $[\boldsymbol{e}_k^{\mathrm{T}}\ \ \overline{\boldsymbol{w}}^{\mathrm{T}}\ \ \overline{\boldsymbol{v}}^{\mathrm{T}}]$ and its transpose, we have

$$\boldsymbol{e}_k^{\mathrm{T}}\boldsymbol{e}_k \leq \mu_l\lambda_l V_k + \mu_l((\mu_w - \gamma_l)\overline{\boldsymbol{w}}^{\mathrm{T}}\overline{\boldsymbol{w}} + (\mu_v - \gamma_l)\overline{\boldsymbol{v}}^{\mathrm{T}}\overline{\boldsymbol{v}}) \tag{33}$$

Finally, substituting (31) into (33) yields

$$\boldsymbol{e}_k^{\mathrm{T}}\boldsymbol{e}_k \leq \mu_l\lambda_l(1-\lambda_l)^k V_0 + \mu_l(\mu_w\overline{\boldsymbol{w}}^{\mathrm{T}}\overline{\boldsymbol{w}} + \mu_v\overline{\boldsymbol{v}}^{\mathrm{T}}\overline{\boldsymbol{v}}) \tag{34}$$

which completes the proof.

Remark 1. For any real matrix $\boldsymbol{M} \in [\underline{\boldsymbol{M}}, \overline{\boldsymbol{M}}] \subseteq \mathbb{R}^{n_x \times n_x}$, there exists an equivalent representation in terms of a convex combination of vertex matrices:

$$\boldsymbol{M} = \textstyle\sum_{i=1}^{N} \boldsymbol{\tau}(i)\boldsymbol{M}_i,\ \sum_{i=1}^{N}\boldsymbol{\tau}(i) = 1,\ \boldsymbol{\tau}(i) \geq 0,\ N = 2^{n_x^2 - \phi} \tag{35}$$

where $\boldsymbol{M}_i$ denotes a vertex matrix whose entries are selected from the corresponding entries of $\underline{\boldsymbol{M}}$ and $\overline{\boldsymbol{M}}$, namely, $\boldsymbol{M}_i(j_1, j_2) \in \{\underline{\boldsymbol{M}}(j_1, j_2), \overline{\boldsymbol{M}}(j_1, j_2)\}$, ϕ represents the number of corresponding equal elements in $\underline{\boldsymbol{M}}$ and $\overline{\boldsymbol{M}}$. Thus, by substituting (35) into (19) and employing the S-procedure, addressing the set-valued problem (related to the presence of the interval variable $\boldsymbol{M}$) in (19) is equivalent to solving:

$$\begin{aligned} &For\ all\ i = 1, \ldots, N \\ &\begin{bmatrix} \boldsymbol{\Phi}_{11,i} & * & * & * & * & * \\ -a\boldsymbol{I} & -b\boldsymbol{I}_{n_x} & * & * & * & * \\ \boldsymbol{0} & \boldsymbol{0} & -\gamma_l\boldsymbol{I}_{n_w} & * & * & * \\ \boldsymbol{0} & \boldsymbol{0} & \boldsymbol{0} & -\gamma_l\boldsymbol{I}_{n_v} & * & * \\ \boldsymbol{\Phi}_{51} & \boldsymbol{P} & \boldsymbol{P}\boldsymbol{D}_1 & -\boldsymbol{W}\boldsymbol{D}_2 & -\boldsymbol{P} & * \\ \boldsymbol{U}\boldsymbol{J}_i & \boldsymbol{0} & \boldsymbol{0} & \boldsymbol{0} & \boldsymbol{0} & \boldsymbol{\Phi}_{66} \end{bmatrix} \prec \boldsymbol{0}, \end{aligned} \tag{36}$$

where $\boldsymbol{\Phi}_{11,i} = \lambda_l\boldsymbol{P} - \boldsymbol{P} + a(\boldsymbol{M}_i + \boldsymbol{M}_i^{\mathrm{T}})$. Therefore, the optimization problem formulated in (22) can be equivalently reformulated as follows:

$$\min_{a,b,\gamma_l,\mu_w,\mu_v,\boldsymbol{P},\boldsymbol{W},\boldsymbol{U}} \mu_l \quad \text{s. t.} \quad (36), (19). \tag{37}$$

Notice that similar procedures have been applied in former studies Buciakowski et al. (2017) to solve different kind of problems. The proposed vertex-based formulation may become computationally demanding for general Jacobian bounds. According to (35), the number of vertices is $N = 2^{n_x^2 - \varphi}$, where φ is the number of fixed entries in the Jacobian interval. Hence, the offline LMI design has exponential complexity in the number of uncertain Jacobian entries. This limitation should be taken into account for dense Jacobian intervals. For sparse or structured Jacobians, however, N can be much smaller, as in the illustrative example where $N = 2$.

Remark 2. A simple high-gain-like interpretation can be obtained from the Mean Value theorem. Since $\boldsymbol{f}(\boldsymbol{x}_k) - \boldsymbol{f}(\hat{\boldsymbol{x}}_k) = \boldsymbol{M}_k(\boldsymbol{x}_k - \hat{\boldsymbol{x}}_k) = \boldsymbol{M}_k\boldsymbol{e}_k,\ \boldsymbol{M}_k \in [\underline{\boldsymbol{M}}, \overline{\boldsymbol{M}}]$ and $\rho_M = \max_{\boldsymbol{M}_i \in \mathrm{vert}([\underline{\boldsymbol{M}}, \overline{\boldsymbol{M}}])} \|\boldsymbol{M}_i\|_2$, the disturbance-free error dynamics satisfies $\|\boldsymbol{e}_{k+1}\|_2 \leq (\|\boldsymbol{A} - \boldsymbol{L}\boldsymbol{C}\|_2 + \rho_M)\,\|\boldsymbol{e}_k\|_2$. Thus, choosing $\boldsymbol{L}$ such that $\|\boldsymbol{A} - \boldsymbol{L}\boldsymbol{C}\|_2 + \rho_M < 1$ makes the nominal error dynamics contractive. This condition shows that the observer correction should dominate the worst-case incremental effect of the bounded Jacobian, while the LMIs in Theorem 1 additionally optimize the peak-to-peak performance.

Based on (21) , we have

$$\|\boldsymbol{e}_k\|_2 \leq \varphi_k^2 \Rightarrow |\boldsymbol{e}_k(i)| \leq \varphi_k, i = 1, \ldots, n_x \tag{38}$$

where $\varphi_k = \sqrt{\mu_l(\lambda_l(1-\lambda_l)^k V_0 + \mu_w\overline{\boldsymbol{w}}^{\mathrm{T}}\overline{\boldsymbol{w}} + \mu_v\overline{\boldsymbol{v}}^{\mathrm{T}}\overline{\boldsymbol{v}})}$. Therefore, based on the peak-to-peak performance index, the lower and upper bounds, denoted by $\underline{\boldsymbol{x}}_k^p$ and $\overline{\boldsymbol{x}}_k^p$, respectively, can be computed as follows:

$$\begin{cases} \underline{\boldsymbol{x}}_k^p = \hat{\boldsymbol{x}}_k - \varphi_k\boldsymbol{I}_{n_x}, \\ \overline{\boldsymbol{x}}_k^p = \hat{\boldsymbol{x}}_k + \varphi_k\boldsymbol{I}_{n_x}, \end{cases} i = 1, \ldots, n_x. \tag{39}$$

Although (39) can provide an offline interval estimation, it is less accurate (tight) due to the conservatism introduced by the overestimation of the effect of the nonlinear term Δf_k done by the inequalities in (31)-(33). Thus, we apply zonotope analysis next to obtain tighter interval estimation.

3.2 Online Zonotopic Interval Estimation

Once the observer in (16) is established, zonotope analysis is used to compute an interval estimation containing $\boldsymbol{x}_k$ based on the reachable set of (18) as stated in the following theorem.

Theorem 2. Suppose that the initial state belongs to the initial zonotope $\boldsymbol{x}_0 \in \mathcal{Z}_0 = \langle \hat{\boldsymbol{x}}_0, \boldsymbol{G}_{\boldsymbol{x},0} \rangle$, or equivalently, $\boldsymbol{e}_0 = \boldsymbol{x}_0 - \hat{\boldsymbol{x}}_0 \in \langle \boldsymbol{0}, \boldsymbol{G}_{\boldsymbol{x},0} \rangle$. Then, the actual state vector $\boldsymbol{x}_k$ is included inside the zonotope $\mathcal{Z}_k = \langle \hat{\boldsymbol{x}}_k, \boldsymbol{G}_{\boldsymbol{x},k} \rangle$, and its corresponding interval estimation $[\underline{\boldsymbol{x}}_k^z, \overline{\boldsymbol{x}}_k^z]$ can be calculated as follows:

$$\boldsymbol{G}_{x,k} = [\tilde{\boldsymbol{A}}\boldsymbol{G}_{x,k-1}\ \boldsymbol{T}_{k-1}\ \boldsymbol{D}_1\boldsymbol{G}_w\ \boldsymbol{L}\boldsymbol{D}_2\boldsymbol{G}_v], \tag{40}$$

$$\boldsymbol{T}_{k-1} = [\boldsymbol{D}^c_{[\boldsymbol{J}\boldsymbol{a}]_{k-1}}\ \boldsymbol{D}^s_{[\boldsymbol{J}\boldsymbol{a}]_{k-1}}], \tag{41}$$

$$[\boldsymbol{J}\boldsymbol{a}]_{k-1} = [\boldsymbol{A}]_{k-1}\boldsymbol{G}_{x,k-1}, \tag{42}$$

$$[\boldsymbol{A}]_{k-1} = \frac{\partial \boldsymbol{f}}{\partial \boldsymbol{x}}(\mathcal{Z}_{k-1}), \tag{43}$$

$$\begin{cases} \underline{\boldsymbol{x}}_k^z(i) = \hat{\boldsymbol{x}}_k - \|\boldsymbol{G}_{x,k}(i,:)\|_1, \\ \overline{\boldsymbol{x}}_k^z(i) = \hat{\boldsymbol{x}}_k + \|\boldsymbol{G}_{x,k}(i,:)\|_1 \end{cases}, \ i = 1, \ldots, n_x, \tag{44}$$

$$\boldsymbol{G}_{x,k} = \downarrow_q (\boldsymbol{G}_{x,k}) \tag{45}$$

where the interval matrix $[\boldsymbol{A}]_{k-1}$ is obtained by replacing the zonotopes $\mathcal{Z}_{k-1}$ in $\frac{\partial \boldsymbol{f}}{\partial \boldsymbol{x}}(\mathcal{Z}_{k-1})$ with their interval outer approximations, followed by interval arithmetic. The basic principles of interval arithmetic are provided in Jaulin et al. (2001), and practical implementations are available in tools such as CORA Althoff and Grebenyuk (2016). The matrices $\boldsymbol{D}^c_{[\boldsymbol{J}\boldsymbol{a}]_{k-1}}$ and $\boldsymbol{D}^s_{[\boldsymbol{J}\boldsymbol{a}]_{k-1}}$ are related to $[\boldsymbol{J}\boldsymbol{a}]_{k-1}$ and are computed using (9). The operator $\downarrow_q (\cdot)$ is employed to limit the number of columns in $\boldsymbol{G}_{x,k}$.

First, based on the Lagrange mean value theorem, $\boldsymbol{f}(\boldsymbol{x}_{k-1})$ can be expanded around $\hat{\boldsymbol{x}}_{k-1}$ as

$$\boldsymbol{f}(\boldsymbol{x}_{k-1}) = \boldsymbol{f}(\hat{\boldsymbol{x}}_{k-1}) + \frac{\partial \boldsymbol{f}}{\partial \boldsymbol{x}}(\boldsymbol{x}'_{k-1})(\boldsymbol{x}_k - \hat{\boldsymbol{x}}_{k-1}) \tag{46}$$

where $\boldsymbol{x}'_{k-1}$ is a point between $\boldsymbol{x}_{k-1}$ and $\hat{\boldsymbol{x}}_{k-1}$, and it is contained in $\mathcal{Z}_{k-1}$.

Substituting (46) into (18), we have

$$\begin{aligned}\boldsymbol{e}_k = \tilde{\boldsymbol{A}}(\boldsymbol{x}_{k-1} - \hat{\boldsymbol{x}}_{k-1}) + \frac{\partial \boldsymbol{f}}{\partial \boldsymbol{x}}(\boldsymbol{x}'_{k-1})(\boldsymbol{x}_{k-1} - \hat{\boldsymbol{x}}_{k-1}) \\ + \boldsymbol{D}_1\boldsymbol{w}_{k-1} - \boldsymbol{L}\boldsymbol{D}_2\boldsymbol{v}_{k-1}\end{aligned} \tag{47}$$

By substituting the variables in (46) with their zonotopic set counterparts, one obtains

$$\begin{aligned}\boldsymbol{e}_k \in \tilde{\boldsymbol{A}}(\mathcal{Z}_{k-1} - \hat{\boldsymbol{x}}_{k-1}) \oplus \frac{\partial \boldsymbol{f}}{\partial \boldsymbol{x}}(\mathcal{Z}_{k-1})(\mathcal{Z}_{k-1} - \hat{\boldsymbol{x}}_{k-1}) \\ \oplus \boldsymbol{D}_1\mathcal{W} \oplus \boldsymbol{L}\boldsymbol{D}_2\mathcal{V}\end{aligned} \tag{48}$$

Based on Property 1, (48) is equivalent to

$$\begin{aligned}\boldsymbol{e}_k \in& \tilde{\boldsymbol{A}}(\langle \hat{\boldsymbol{x}}_{k-1}, \boldsymbol{G}_{x,k-1}\rangle - \hat{\boldsymbol{x}}_{k-1}) \\ &\oplus \frac{\partial \boldsymbol{f}}{\partial \boldsymbol{x}}(\mathcal{Z}_{k-1})(\langle \hat{\boldsymbol{x}}_{k-1}, \boldsymbol{G}_{x,k-1}\rangle - \hat{\boldsymbol{x}}_{k-1}) \\ &\oplus \boldsymbol{D}_1\langle \boldsymbol{0}, \boldsymbol{G}_w\rangle \oplus \boldsymbol{L}\boldsymbol{D}_2\langle \boldsymbol{0}, \boldsymbol{G}_v\rangle \\ \in& \tilde{\boldsymbol{A}}\langle \boldsymbol{0}, \boldsymbol{G}_{x,k-1}\rangle \oplus [\boldsymbol{J}\boldsymbol{a}]_{k-1}\langle \boldsymbol{0}, \boldsymbol{G}_{x,k-1}\rangle \\ &\oplus \boldsymbol{D}_1\langle \boldsymbol{0}, \boldsymbol{G}_w\rangle \oplus \boldsymbol{L}\boldsymbol{D}_2\langle \boldsymbol{0}, \boldsymbol{G}_v\rangle \\ &\oplus \langle \boldsymbol{0}, \boldsymbol{D}_1\boldsymbol{G}_w\rangle \oplus \langle \boldsymbol{0}, \boldsymbol{L}\boldsymbol{D}_2\boldsymbol{G}_v\rangle\end{aligned} \tag{49}$$

Then, we apply Lemma 2 to $\langle \boldsymbol{0}, [\boldsymbol{J}\boldsymbol{a}]_{k-1}\boldsymbol{G}_{x,k-1}\rangle$, which leads to

$$\Diamond\langle \boldsymbol{0}, [\boldsymbol{J}\boldsymbol{a}]_{k-1}\boldsymbol{G}_{x,k-1}\rangle = \langle \boldsymbol{0}, \boldsymbol{T}_{k-1}\rangle \tag{50}$$

where $\boldsymbol{T}_{k-1} = [\boldsymbol{D}^c_{[\boldsymbol{J}\boldsymbol{a}]_{k-1}} \ \boldsymbol{D}^s_{[\boldsymbol{J}\boldsymbol{a}]_{k-1}}]$. Substituting (50) into (49), we obtain

$$\boldsymbol{e}_k \in \langle \boldsymbol{0}, \boldsymbol{G}_{x,k}\rangle \tag{51}$$

$$\boldsymbol{G}_{x,k} = [\tilde{\boldsymbol{A}}\boldsymbol{G}_{x,k-1} \ \boldsymbol{T}_{k-1} \ \boldsymbol{D}_1\boldsymbol{G}_w \ \boldsymbol{L}\boldsymbol{D}_2\boldsymbol{G}_v] \tag{52}$$

Last, according to (17) and (51), it follows

$$\boldsymbol{x}_k = \hat{\boldsymbol{x}}_k + \boldsymbol{e}_k \in \langle \hat{\boldsymbol{x}}_k, \boldsymbol{G}_{x,k}\rangle \subseteq [\underline{\boldsymbol{x}}^z_k, \overline{\boldsymbol{x}}^z_k] \tag{53}$$

The lower bound $\underline{\boldsymbol{x}}^z_k$ and upper bound $\overline{\boldsymbol{x}}^z_k$ can be computed by (6), which completes the proof.

3.3 Comprehensive method

Combining the interval estimation (39) provided by bounded-error and the interval estimation (44) obtained by zonotope analysis, the bounds of the comprehensive interval estimation are computed as follows:

$$\begin{cases}\underline{\boldsymbol{x}}_k = \max(\underline{\boldsymbol{x}}^p_k, \underline{\boldsymbol{x}}^z_k), \\ \overline{\boldsymbol{x}}_k = \min(\overline{\boldsymbol{x}}^p_k, \overline{\boldsymbol{x}}^z_k),\end{cases} \tag{54}$$

where $\underline{\boldsymbol{x}}_k \in \mathbb{R}^{n_x}$ and $\overline{\boldsymbol{x}}_k \in \mathbb{R}^{n_x}$ are the lower bound and upper bound of state $\boldsymbol{x}_k$, respectively.

Remark 3. The proposed method is also applicable to linear systems with an uncertain matrix $\boldsymbol{A} \in \hat{\boldsymbol{A}} + [\Delta\boldsymbol{A}]$ by defining $\boldsymbol{f}(\boldsymbol{x}_k) \triangleq \Delta\boldsymbol{A}\boldsymbol{x}_k$, where $\hat{\boldsymbol{A}}$ is a real-valued matrix and $[\Delta\boldsymbol{A}]$ is an interval matrix. If $\Delta\boldsymbol{A} \in [\underline{\boldsymbol{M}}, \overline{\boldsymbol{M}}]$, then Assumption 1 is satisfied with $\frac{\partial \boldsymbol{f}}{\partial \boldsymbol{x}} = \Delta\boldsymbol{A}$, and no additional design is required.

4. ILLUSTRATIVE EXAMPLE

The effectiveness of the proposed interval estimation method is demonstrated through the following example:

Consider the nonlinear pendulum model in Tahir and Açıkmeşe (2021):

$$\begin{cases}\boldsymbol{x}_{k+1} = \boldsymbol{A}\boldsymbol{x}_k + \boldsymbol{f}(\boldsymbol{x}_k) + \boldsymbol{D}_1\boldsymbol{w}_k \\ \boldsymbol{y}_k = \boldsymbol{C}\boldsymbol{x}_k + \boldsymbol{D}_2\boldsymbol{v}_k\end{cases} \tag{55}$$

where $\boldsymbol{A} = \begin{bmatrix}1 & 0.065 \\ 0 & 1\end{bmatrix}$, $\boldsymbol{f}(\boldsymbol{x}_k) = \begin{bmatrix}0 \\ -0.065\sin(\boldsymbol{x}_k(1))\end{bmatrix}$, $\boldsymbol{C} = [1 \ 0]$, $\boldsymbol{D}_1 = \boldsymbol{I}_2$, $\boldsymbol{D}_2 = 0.1$, $\boldsymbol{x} = [x_1 \ x_2]^{\mathrm{T}}$ denotes the position and angular velocity of pendulum. The process disturbance and measurement noise satisfy $\boldsymbol{w}_k \in 0.006\begin{bmatrix}\mathrm{rand}(-1,1) \\ \mathrm{rand}(-1,1)\end{bmatrix}$, $\boldsymbol{v}_k \in 0.01\mathrm{rand}(-1,1)$ with $\mathrm{rand}(-1,1)$ means an independent random signal uniformly distributed over $[-1,1]$. The lower bound $\underline{\boldsymbol{M}}$ and upper bound $\overline{\boldsymbol{M}}$ of the Jacobian matrix are $\underline{\boldsymbol{M}} = \begin{bmatrix}0 & 0 \\ -0.065 & 0\end{bmatrix}$, $\overline{\boldsymbol{M}} = \begin{bmatrix}0 & 0 \\ 0.065 & 0\end{bmatrix}$. Based on (35), the number of $\boldsymbol{M}_i$ can be computed as $N = 2^{2^2-3} = 2$. Then, setting $\lambda = 0.5$ and solving the optimization problem (37), we obtain $\mu_w = 15.7$, $\mu_v = 15.7$, $\varphi_0 = 1.15$ and $\boldsymbol{L} = [1.503 \ 7.737]^{\mathrm{T}}$. Moreover, we set the initial state at $\boldsymbol{x}_0 = [1, \ 0]$, the initial state vector of the observer $\hat{\boldsymbol{x}}_0 = [0.98, \ 0.02]$, the shape matrices of the considered zonotopes are $\boldsymbol{G}_{x,0} = \mathrm{diag}([0.1 \ \ 1])$, $\boldsymbol{G}_w = 0.006\boldsymbol{I}_2$, $\boldsymbol{G}_v = 0.01$ and $q = 20$. All simulations were performed in MATLAB R2023b on a Windows 11 machine with an Intel i7-12700 CPU and 16 GB RAM. Since the Jacobian interval is sparse, only $N = 2$ vertices are involved. The offline LMI optimization took 0.369 s, while the online zonotope propagation over 50 steps took 0.140 s in total, i.e., 2.754 ms per step on average.

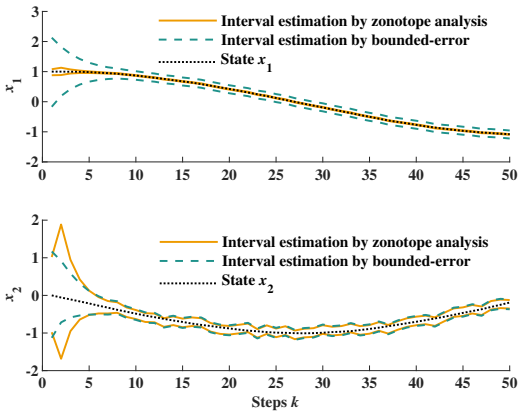


Fig. 1. The interval estimation by zonotope analysis and bounded-error

The obtained simulation results by the proposed set-valued state estimators are shown in Fig. 1. In Fig. 1, the dotted lines stand for the actual state. The solid lines and the dashed ones correspond to the interval estimation by zonotope analysis (Eq. (44)) and bounded-error method (Eq. (39)), respectively. Thanks to the use of inequality relaxations in the observer design process, zonotope analysis can provide tighter interval estimation than the bounded-error approach. However, one observes that for the unmeasured state variable, the convergence rate of the bounded-error method is faster than the zonotope analysis approach.

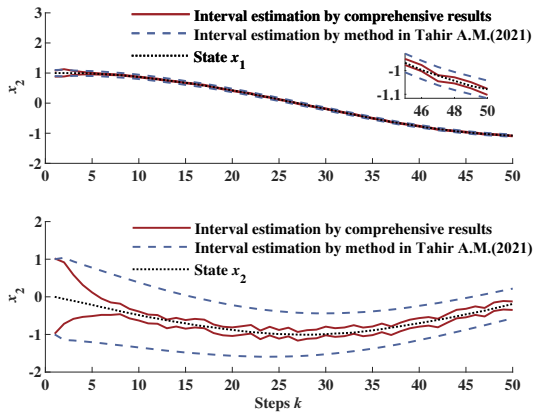


Fig. 2. The interval estimation by comprehensive results and existing method

The comprehensive results (Eq. (54)) make a good balance between estimation accuracy and convergence rate. The interval estimation obtained by comprehensive approach and the method in Tahir and Açıkmeşe (2021) is presented in Fig. 2. In Fig. 2, the dotted lines stand for the actual state. The solid lines and the dashed ones correspond to the interval estimation by comprehensive approach and the method in Tahir and Açıkmeşe (2021). The simulation results indicate that the proposed method outperforms the existing approach Tahir and Açıkmeşe (2021). In particular, it achieves quicker convergence and provides a more precise estimation interval.

5. CONCLUSIONS

A comprehensive interval estimation method is proposed for discrete-time bounded Jacobian nonlinear systems subjected to unknown but bounded disturbance and noise. First, a bounded-error method is developed based on a robust observer, which is designed to guarantee the peak-to-peak estimation performance index. Then, a comprehensive interval estimation method is proposed by combining bounded-error information and zonotopic interval estimation obtained from extending zonotope set computation to the dynamics of the estimation error. Finally, simulation results have shown the effectiveness of the developed approach. Extending the proposed method to achieve the fault detection and isolation will be our future works.

APPENDIX

5.1 Size reduction operator

Let $\overrightarrow{\boldsymbol{G}}$ denote the matrix obtained by sorting the columns of $\boldsymbol{G} \in \mathbb{R}^{n\times m}$ in descending order according to their Euclidean norms. The reduction operator is defined as $\downarrow_q (\boldsymbol{G}) = [\boldsymbol{G}_1, \boldsymbol{G}_2]$, where $\boldsymbol{G}_1$ contains the first $q-n$ columns of $\overrightarrow{\boldsymbol{G}}$, and $\boldsymbol{G}_2$ is a diagonal matrix whose diagonal entries are given by

$$\boldsymbol{G}_2(i,i) = \sum_{j=q-n+1}^{m} \left|\overrightarrow{\boldsymbol{G}}(i,j)\right|, \quad i = 1,\ldots,n.$$

It should be noted that the reduction operation restricts the number of columns in the generator matrix, but at the cost of introducing additional conservatism.

REFERENCES

Alamo, T., Bravo, J.M., and Camacho, E.F. (2005). Guaranteed state estimation by zonotopes. *Automatica*, 41(6), 1035–1043.

Althoff, M. and Grebenyuk, D. (2016). Implementation of interval arithmetic in CORA 2016. In *Proc. of the 3rd International Workshop on Applied Verification for Continuous and Hybrid Systems*, 91–105.

Althoff, M. and Rath, J.J. (2021). Comparison of guaranteed state estimators for linear time-invariant systems. *Automatica*, 130, 109662.

Boyd, S.P. and Vandenberghe, L. (2004). *Convex optimization*. Cambridge university press.

Buciakowski, M., Witczak, M., Puig, V., Rotondo, D., Nejjari, F., and Korbicz, J. (2017). A bounded-error approach to simultaneous state and actuator fault estimation for a class of nonlinear systems. *Journal of Process Control*, 52, 14–25.

De Oliveira, M.C., Bernussou, J., and Geromel, J.C. (1999). A new discrete-time robust stability condition. *Systems & control letters*, 37(4), 261–265.

Efimov, D., Perruquetti, W., Raïssi, T., and Zolghadri, A. (2013). On interval observer design for time-invariant discrete-time systems. In *2013 European Control Conference (ECC)*, 2651–2656. IEEE.

Jaulin, L., Kieffer, M., Didrit, O., Walter, E., Jaulin, L., Kieffer, M., Didrit, O., and Walter, É. (2001). *Interval analysis*. Springer.

Khajenejad, M. and Yong, S.Z. (2022). H_∞-optimal interval observer synthesis for uncertain nonlinear dynamical systems via mixed-monotone decompositions. *IEEE Control Systems Letters*, 6, 3008–3013.

Li, J., Wang, Z., Shen, Y., and Wang, Y. (2019). Interval observer design for discrete-time uncertain takagi–sugeno fuzzy systems. *IEEE Transactions on Fuzzy Systems*, 27(4), 816–823.

Raïssi, T., Efimov, D., and Zolghadri, A. (2011). Interval state estimation for a class of nonlinear systems. *IEEE Transactions on Automatic Control*, 57(1), 260–265.

Tahir, A.M. and Açıkmeşe, B. (2021). Synthesis of interval observers for bounded Jacobian nonlinear discrete-time systems. *IEEE Control Systems Letters*, 6, 764–769.

Tang, W., Wang, Z., Wang, Y., Raïssi, T., and Shen, Y. (2019). Interval estimation methods for discrete-time linear time-invariant systems. *IEEE Transactions on Automatic Control*, 64(11), 4717–4724.

Tang, W., Wang, Z., Zhang, Q., and Shen, Y. (2020). Set-membership estimation for linear time-varying descriptor systems. *Automatica*, 115, 108867.

Wang, Y., Wang, Z., Puig, V., and Cembrano, G. (2018). Zonotopic set-membership state estimation for discrete-time descriptor lpv systems. *IEEE Transactions on Automatic Control*, 64(5), 2092–2099.

Wang, Z. and Shen, Y. (2023). *Model-Based Fault Diagnosis*. Springer.

Wang, Z., Zhang, L., Ra, T., Shen, Y., et al. (2024). Interval estimation for discrete-time Takagi-Sugeno fuzzy nonlinear systems with parameter uncertainties. *IEEE Transactions on Fuzzy Systems*.

Zhang, W., Wang, Z., Raïssi, T., and Shen, Y. (2021). Ellipsoid-based interval estimation for lipschitz nonlinear systems. *IEEE Transactions on Automatic Control*, 67(12), 6802–6809.